

## Article

# Design of High Peak Power Pulsed Laser Diode Driver

Ching-Yao Liu <sup>1</sup>, Chih-Chiang Wu <sup>2</sup>, Li-Chuan Tang <sup>1</sup>, Wei-Hua Chieng <sup>1,\*</sup>, Edward-Yi Chang <sup>3</sup>, Chun-Yen Peng <sup>4</sup> and Hao-Chung Kuo <sup>4</sup>

<sup>1</sup> Department of Mechanical Engineering, College of Engineering, National Yang Ming Chiao Tung University, Hsinchu 30010, Taiwan

<sup>2</sup> Mechanical and Mechatronics Systems Research Laboratories, Industrial Technology Research Institute, Hsinchu 31040, Taiwan

<sup>3</sup> Department of Material Science and Engineering, College of Engineering, National Yang Ming Chiao Tung University, Hsinchu 30010, Taiwan

<sup>4</sup> Semiconductor Research Center, Hon Hai Research Institute, Taipei 114699, Taiwan

\* Correspondence: cwh@nycu.edu.tw; Tel.: +886-3-571-2121 (ext. 55152)

**Abstract:** This paper attempts to describe a laser diode driver circuit using the depletion mode gallium nitride high electron mobility transistor (D-mode GaN HEMT) to generate nanosecond pulses at a repetition rate up to 10 MHz from the vertical-cavity surface-emitting laser (VCSEL). The feature of this driver circuit is a large instantaneous laser power output designed in the most efficient way. The design specifications include a pulse duration between 10 ns and 100 ns and a peak power up to above 100 W. The pulsed laser diode driver uses the D-mode GaN HEMT, which has very small  $C_{oss}$  difference between turn-on and turn-off states. The analysis is according to a laser diode model that is adjusted to match the VCSEL, made in National Yang Ming Chiao Tung University (NYCU). A design guide is summarized from the derivations and analysis of the proposed laser diode driver. According to the design guide, we selected the capacitor, resistor, and diode components to achieve 10 ns to 100 ns pulse duration for laser lighting. The experiment demonstrated that the maximum power-to-light efficiency can be as high as 86% and the maximum peak power can be 150 W, which matches the specifications of certain applications such as light detection and ranging (LiDAR).



**Citation:** Liu, C.-Y.; Wu, C.-C.; Tang, L.-C.; Chieng, W.-H.; Chang, E.-Y.; Peng, C.-Y.; Kuo, H.-C. Design of High Peak Power Pulsed Laser Diode Driver. *Photonics* **2022**, *9*, 652. <https://doi.org/10.3390/photonics9090652>

Received: 27 July 2022

Accepted: 11 September 2022

Published: 14 September 2022

**Publisher's Note:** MDPI stays neutral with regard to jurisdictional claims in published maps and institutional affiliations.



**Copyright:** © 2022 by the authors. Licensee MDPI, Basel, Switzerland. This article is an open access article distributed under the terms and conditions of the Creative Commons Attribution (CC BY) license (<https://creativecommons.org/licenses/by/4.0/>).

**Keywords:** laser driver; high peak power; laser diode model; VCSEL

## 1. Introduction

LiDAR is widely used in autonomous cars [1], unmanned aerial vehicles (UAVs) [2], and forest science [3]; it sends out a pulse laser signal and simultaneously gathers the information of the reflection from objects. The object distance is calculated by the optical time-of-flight (TOF) [4], thus the higher the laser peak current, or power, pulses means farther detection can be achieved, and shorter pulse duration represents better detection accuracy. For some applications, such as simultaneous localization and mapping (SLAM) [5], we additionally need a high measurement sampling rate to acquire enough information.

Two laser driver topologies, including the laser diode being in parallel [6] and series [7] with a transistor, have been introduced in the literature. The series topology is featured with a simple circuit, whereas the parallel one is characterized by high optical power and short pulses [8,9]. Some researchers integrated the power switch with its driver using CMOS technology in order to operate at megahertz frequency [7,10]; however, high switching frequency leads to more switching loss for conventional silicon-based materials. The methodology introduced in [11] uses a momentary boost in supply voltage to reduce power overhead and thus improves the power efficiency. Furthermore, some other researchers [12,13] used wide bandgap devices such as the GaN HEMT for the laser driver application due to their low products of total gate charge and conduction resistance. The wide bandgap devices implemented in laser drivers yield better compactness and

power efficiency than that of MOSFET [13]. In recent years, EPC Co. have published a laser driver with an enhancement mode power GaN device that is capable of driving a laser with current pulses, with total pulse widths as short as 1.2 ns and currents of up to 28A [14].

Aside from the aforementioned advantages, GaN devices have other superior material properties, such as zero reverse recovery and low output capacitance difference between turn-on and turn-off of the transistor [15,16]. There are also challenges using D-mode GaN, for example, a negative voltage is required to be applied at the gate to turn off the normally on channel. To overcome the aforementioned challenges, several schemes [17–19] have transformed the normally on device into a normally off transistor with the charge pump gate drives [17], the cascode GaN structure [18], and the self-powered gate drives [19]. As the laser driving frequency is limited by the inductance of the laser and the capacitance of the driver system, we will need to reduce the parasitic inductance on the circuit board and use GaN HEMT to reduce the parasitic capacitance for higher repetition rate and shorter pulse duration [6].

In addition, high power laser emitters are critical to the LiDAR system, of which VCSEL is used mostly in high speed optical applications such as 3D sensing and light detection and ranging [20,21]. With large current density, directive emission, low divergence angle, narrow bandwidth, and low power consumption, VCSEL has become one of the most reliable and high performance lasers [22–24]. Some studies about the analysis of laser equivalent circuit models [25–28] considering the resonance mechanism [25], rate equations [26], contact resistance equation [27], and thermal equation [28] can yield simulation results approaching the real phenomenon.

The aim of this paper is to propose a laser driver with D-mode GaN HEMT that is capable of generating high peak power pulse within nanoseconds to VCSEL for a LiDAR system. With feedback control of pre-boosted supply voltage, the presented laser driver will yield high peak power under high power efficiency. Section 2 depicts the laser diode and the VCSEL equivalent circuit model used in this research according to rate equations and the resonance phenomenon. In Section 3, the proposed high power laser driver for VCSEL is discussed, including pre-boosted power supply and analysis of laser circuit response. The design guide for the D-mode GaN based laser driver that provides power to light efficiency improvement and high peak power is presented in Section 4. The proposed laser driver with D-mode GaN and VCSEL is verified through the PSPICE simulation and experiment. The estimation of total power received by the photodetector is shown in Section 5. The conclusion of this work is summarized in Section 6.

## 2. Laser Diode

For the circuit analysis and simulation laser diode driving, we need to obtain the circuit response instead of the laser response. Thus, the equivalent circuit needs to be used to predict the waveforms of the current and voltage using circuit simulation software. As shown in Figure 1, within the maximum power rating region, the P-I curve distinguishes the spontaneous emission (LED light emitting) region from the stimulated emission (laser oscillating) region; the current level that triggers laser oscillation is the threshold current. The slope efficiency is almost constant in the stimulated emission region.

As shown in Figure 2, the major term of the current source of the PIN diode [27] can be modeled into a temperature dependent function as follows. Table 1 shows the parameters used in circuit analysis, which includes different stray inductances when using matrix board and printed circuit board (PCB).

$$I_{LD} = AT^n e^{\frac{v_D - E_b}{V_T}} = \left( AT^n e^{\frac{-E_b}{V_T}} \right) e^{\frac{v_D}{V_T}} \quad (1)$$

where  $E_b$  denotes band gap potential of the semiconductor in volts,  $n$  denotes temperature exponent, and  $A$  is a constant independent of the temperature  $T$ . It is modelled into a similar form as a normal PN diode as follows.

$$I_{LD} = I_{SS} \left( e^{\frac{v_D}{NVT}} - 1 \right) \tag{2}$$

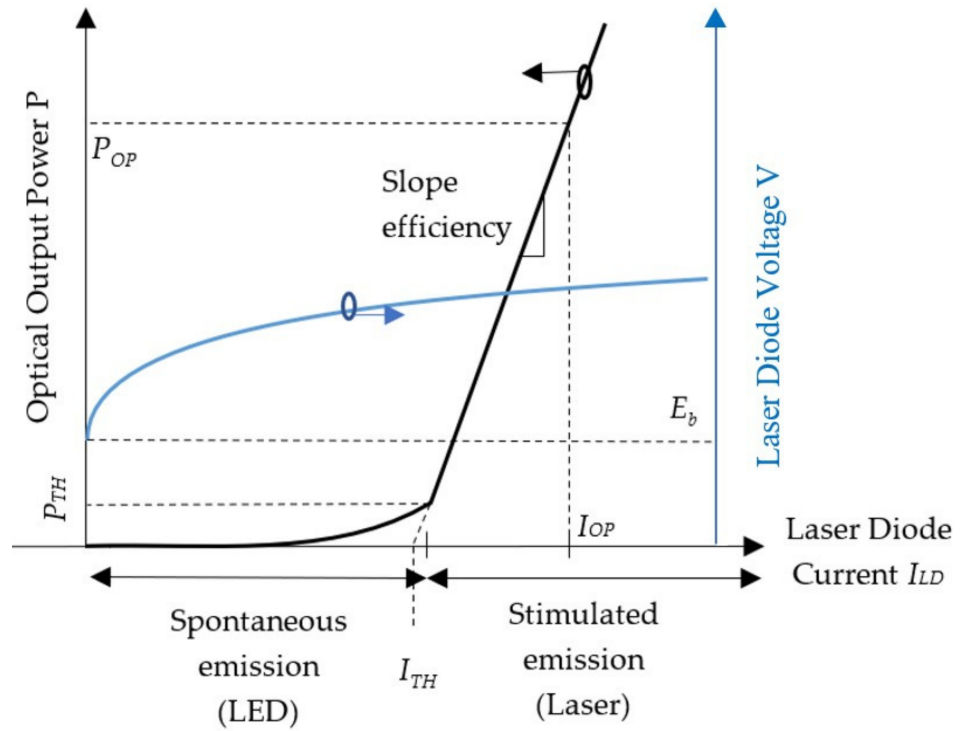
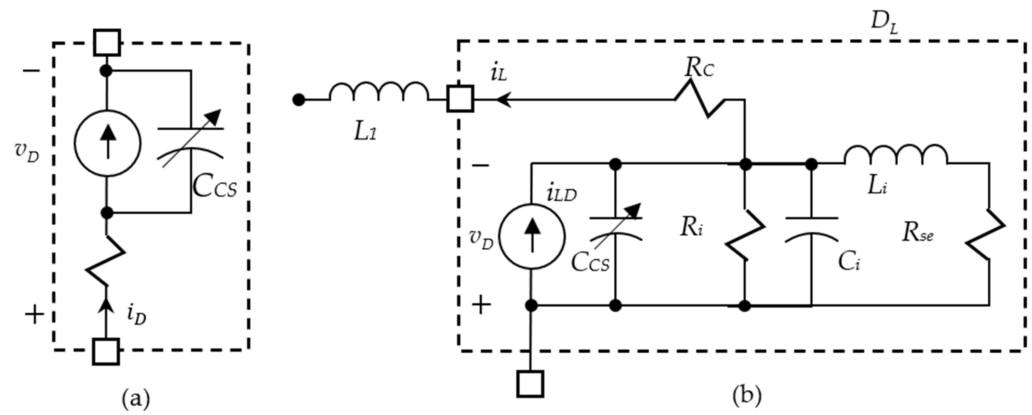


Figure 1. P-I curve and V-I curve of laser diode.

Table 1. Parameters used in laser diode circuit modeling.

Symbol	Unit	Value
$V_J$	V	1.9
$C_{sc(o)}$	pF	0.6
$C_i$	pF	400
$R_i$	$\Omega$	3.0
$L_i$	nH	30
$L_1$	nH	Matrix board PCB 100 20
$R_{se}$	m $\Omega$	100
$M$		0.5
$N$		1
$E_b$	V	1.9
$I_{ss}$	A	$1 \times 10^{-18}$
$C_1$	$\mu$ F	220
$R_1$	$\Omega$	100
$R_2$	$\Omega$	100
$T_1$	$\mu$ s	44



**Figure 2.** Circuit model for (a) diode and (b) VCSEL (940 nm by NYCU or V3-7-2000-S by EGISMOS) laser diode.

It may be substituted with  $N = 1$  and the reverse saturation current as follows.

$$I_{SS} = AT^n e^{\frac{-E_b}{V_T}} \tag{3}$$

where  $E_b$  denotes the band gap potential of the laser diode in volts. This capacitance named the space-charge capacitance,  $C_{SC}$ , of the active region is given as follows.

$$C_{SC} = C_{SC(0)} \left(1 - \frac{v_D}{V_J}\right)^{-M} \tag{4}$$

where  $C_{sc(0)}$  is the zero-bias space-charge capacitance and  $V_J$  is the heterojunction built-in potential. The active layer diffusion capacitance of the laser diode is  $C_i$ . The inductance  $L_i$  arises from the small signal analysis of the rate equations and represents the resonance phenomenon of the laser diode with capacitance  $C_i$ . The resistance  $R_i$  includes the differential resistance of the laser diode model damping due to the spontaneous and stimulated recombination terms in the rate equations. The resistance  $R_{se}$  models damping due to spontaneous emission coupled into the lasing mode. In the equivalent circuit we model both  $R_i$  and  $R_{se}$  together into  $R_{i,se}$ ;  $R_c$  is the contact resistance, which includes the semiconductor bulk resistance. The main contribution to  $R_c$  comes from the contacts because the bulk resistance of semiconductors is very low. The inductance  $L_1$  arises from the circuit parasitic inductance, which is always preferred to be as low as possible.

### 3. VCSEL Laser Diode Driver

Commercial circuitry to switch on the laser is EPC9144 [14], which is simplified as shown in Figure 3a. The capacitor  $C_b$  is 1 nF, which serves as a line filter. When  $v_{GS}$  is high, the transistor  $M_1$  turns on, and the current flows from the voltage source through a very small resistance  $R_1$  to the laser diode. The reverse saturation current  $I_{SS}$  on the laser diode is a function of temperature when the temperature of the laser diode increases the diode current  $i_{LD}$  derived in Equation (1) and cannot be ignored [27] at a constant temperature operation. The moment when  $v_{DS}$  goes to zero is the time when the laser diode goes into the stimulated emission mode, and the rest of the oscillating response is the resonance phenomenon of the laser diode when the laser diode is likely to be in the spontaneous emission mode. The signals are taken from the transistor as shown in Figure 3b. When the gate-source voltage is operated with an on-time duration 10 ns at a pulse repetition rate 10 kHz, the transistor  $M_1$  turns on and  $v_{DS}$  drops to low voltage. The actual  $i_{LD}$  can be roughly estimated through dividing the voltage difference  $V_{DD} - v_{DS}$  by the dynamic  $R_{on}$  resistance of the GaN HEMT.

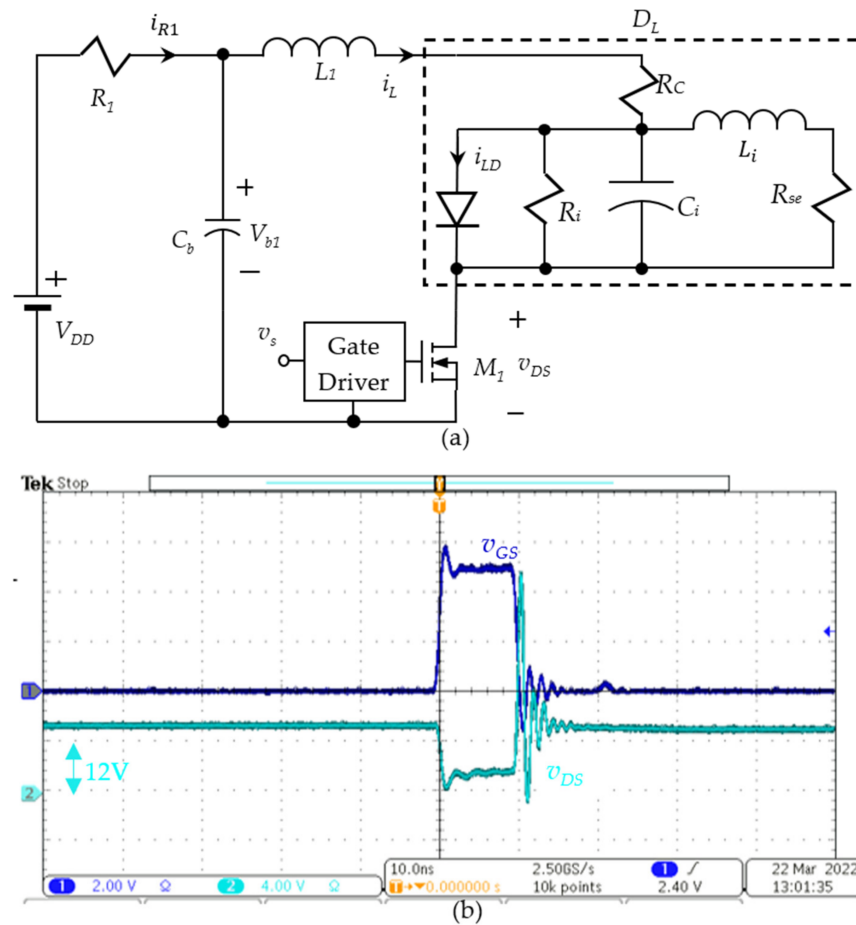


Figure 3. EPC9144 (a) schematic and (b) waveforms with repetition rate 10 kHz and time duration 10 ns.

The drawback of the circuit in Figure 3a is the resistor  $R_1$  must be high enough to reduce the voltage ringing, as shown in Figure 3b, when the transistor  $M_1$  turns off. The high resistance  $R_1$  limits the current  $i_{LD}$  flowing through the diode, which is typically ten times higher than the contact resistance  $R_c$ . For the high peak laser power application, the circuit must be reconsidered.

### 3.1. The Proposed VCSEL Laser Diode Driver

There is a need to adjust the current level of driving due to different selections of lighting in a number of groups of laser diodes. Therefore, a boost converter used to escalate the voltage level of the capacitor is proposed and shown in Figure 4.

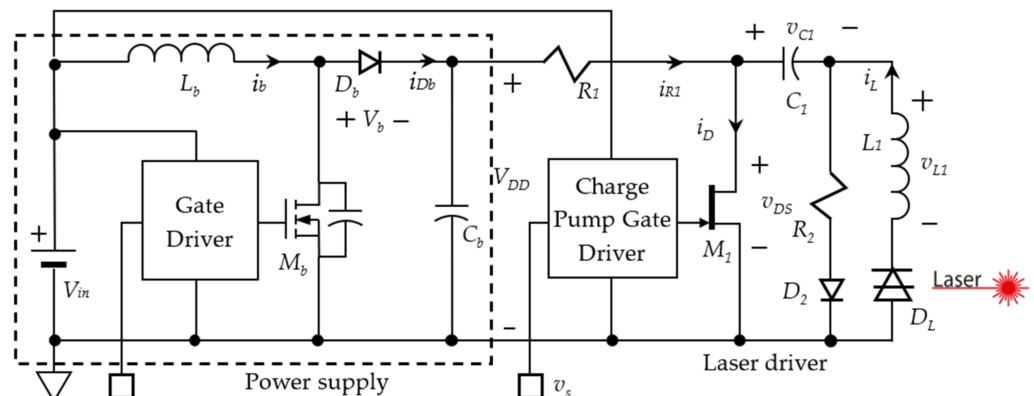


Figure 4. D-mode GaN HEMT laser driver.

### 3.2. Power Supply

The boost switching power supply is used to control the input voltage  $v_{DD}$  for the laser driver circuit from a low voltage, such as  $V_{in} = 4\text{ V}$  from Li-ion battery. The boost power supply is used to boost the low voltage into a high voltage for the laser. The input voltage  $v_{DD}$  is then subsequently charging the capacitor  $C_1$ , which is the main voltage source in the laser lighting loop. On the power supply side, the boost converter circuit consists of an inductor  $L_b$ , diode  $D_b$ , transistor  $M_b$ , and capacitor  $C_b$ . The diode  $D_b$  comes into the reverse bias when the transistor  $M_b$  is switched on. During the  $M_b$  turn-on period  $\delta_b T_b$ , the inductor  $L_b$  increases its magnetic energy with a current rise as follows.

$$\Delta I_b = \frac{V_{in} \delta_b T_b}{L_b} \tag{5}$$

This magnetic energy will be conveyed to the capacitor  $C_b$  during its  $M_b$  turn-off period. Because the output current from the power supply to the laser driver is very low, the boost converter working in the discontinuous current mode is assumed. On the path of the current flowing from the inductor  $L_b$  to the capacitor  $C_b$ , the diode  $D_b$  is forced into a forward bias. The charging current of the capacitor  $C_b$  is derived in the steady state as follows.

$$\Delta I_b = \frac{(V_{DD} - V_{in}) \alpha (1 - \delta_b) T_b}{L_b} \tag{6}$$

where  $\alpha$ ,  $0 \leq \alpha \leq 1$ , denotes the fraction of the current flowing time from the  $M_b$  turn-off period  $(1 - \delta_b) T_b$ . During the  $M_b$  turn-off period, the current  $i_{D_b}$  flows into the capacitor  $C_b$  through the diode  $D_b$ .

$$\alpha = \frac{2}{(1 - \delta_b) \Delta I_b} I_{R1} = \frac{2}{(1 - \delta_b) \Delta I_b} \frac{P_L}{V_b} \tag{7}$$

The term  $V_{DD}$  denotes the average voltage across the capacitor  $C_b$ ;  $I_{R1}$  denotes the average current flow through resistor  $R_1$ ;  $P_L$  denotes the power loss in the laser diode driver including the resistor  $R_1$ . Substituting Equation (7) into (6) and comparing Equations (5) and (6), we have the capacitor voltage  $v_{DD}$  as follows.

$$\delta_b = \sqrt{\frac{2P_L L_b}{V_{in}^2 T_b} \left(1 - \frac{V_{in}}{V_{DD}}\right)} \tag{8}$$

It is observed that the capacitor voltage is irrelevant to the capacitance when the boost converter stands alone. However, when we considered the current output  $i_{R1}$  from  $R_1$ , the capacitor voltage  $v_{DD}$  is charged/discharged by two sources, and the total voltage can be calculated from the superposition theorem as follows.

$$v_{DD} = V_{DD} - \Delta v_{DD} = V_{DD} - \frac{\Delta Q}{C_b} \tag{9}$$

The capacitor voltage is then a function of the capacitance of  $C_b$  and the charge withdrawn  $\Delta Q$  from the capacitor. On the laser driver side, the capacitor  $C_1$  obtains the charges from capacitor  $C_b$  when transistor  $M_1$  turns off. The charge redistribution between two capacitors occurs when transistor  $M_b$  turns on, and the diode  $D_b$  is under reverse bias.

$$\frac{\Delta v_{DD}}{\Delta v_{C1}} = \frac{C_1}{C_b} \tag{10}$$

The steady state of  $v_{C1}$  is obtained when the charge redistribution is completed. The time constant may be seen as the capacitor  $C_b$  to charge the  $C_1$ , which, relatively, has a

very small capacitance. The governing equation for the charge redistribution is derived as follows.

$$\frac{dv_{C1}}{dt} + \frac{1}{(R_1 + R_2)C_1}v_{C1} = \frac{V_{DD}}{(R_1 + R_2)C_1} \tag{11}$$

In order to reduce the complexity for the analysis, one may reduce charging time constant  $T_1$  of capacitor  $C_1$ . The capacitor loses electrical energy  $\Delta E$  each time when the laser diode is powered up within the pulse train period  $T_{pp}$ . Assuming that  $V_{C1} = V_{DD}$  at steady state, we can derive the power loss from the laser diode driver circuit as follows.

$$P_L = \frac{\Delta E}{T_{pp}} = \frac{C_1 V_{DD}}{T_{pp}} \Delta V_{C1} \tag{12}$$

Equation (8) is then written as follows.

$$\delta_b = \sqrt{\Delta v_{C1}} \sqrt{\frac{2L_b C_1}{T_{pp} T_b V_{in}} \left( \frac{V_{DD}}{V_{in}} - 1 \right)} \tag{13}$$

The above equation states that the power supply duty cycle  $\delta_b$  is proportional to the square root of the voltage drop  $\Delta v_{C1}$  in capacitor  $C_1$ .

### 3.3. Laser Circuit Response

The fundamental data of the VCSEL are from a light–current–voltage (LIV) curve, which simultaneously measures the electrical and optical output power characteristics of the device. LIV characteristics are a function of laser temperature as indicated in Equation (6), which must be tightly controlled. The main reasons for performing low-duty-cycle pulsed laser driving are thermal management, thermal response, and transient response. The pulse driving technique is mainly applied to generate nanosecond pulses of high peak power with solid-state bulk lasers. In this study, we are especially interested in the repetition rate of 10 kHz and 1 MHz. As shown in Figure 5, there are four phases in a LIV pulse, namely the switch parasitic capacitor discharge time  $t_{spd}$ , the switch on-time  $t_{on}$ , the switching parasitic charge time  $t_{spc}$ , and the laser diode resonant time  $t_{lr}$ . The entire cycle between two consecutive gate turn-on signals is a pulse period time  $T_{pp}$ , which is the reciprocal of the laser repetition rate.

$$T_{pp} = t_{spd} + t_{on} + t_{spc} + t_{lr} \tag{14}$$

where  $T_{pp}$  is the reciprocal of the repetition rate  $f_{LD}$ , that is

$$T_{pp} = \frac{1}{f_{PD}} \tag{15}$$

The pulse duration achieved is typically in the nanosecond range and usually well above the resonator round-trip time. The pulse duration of the laser pulse is  $t_p$ , which consists of the switch parasitic capacitor discharge time  $t_{spd}$ , the switch on-time  $t_{on}$ .

$$t_p = t_{spd} + t_{on} \tag{16}$$

As a simplified model, the laser lighting time driven by the switch conduction is written as follows.

$$t_{la} = t_{on} + t_{spc} \tag{17}$$

The power of the laser radiation builds up very quickly in the laser resonator. The large cavity power present at that time leads to further depletion of the stored energy during the time where the power decays. Usually, the energy extracted after the pulse maximum is similar to that before the pulse maximum, and the resulting pulse shape is roughly symmetric. The laser diode resonance is due to inductance  $L_i$  with capacitance  $C_i$ . The resonance mechanism of a true laser diode may be more sophisticated than the circuit

model, however, it is simplified into the circuit as shown in Figure 2 and analyzed only for circuit control purposes.

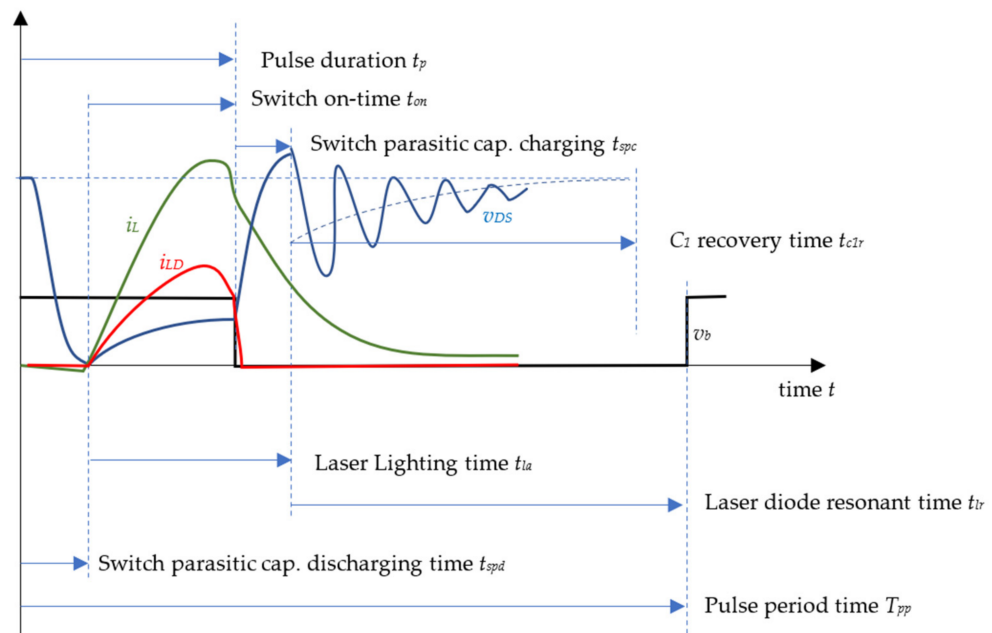


Figure 5. Laser driver circuit response model for short pulse duration.

### 3.3.1. Switch Parasitic Capacitor Discharge Time $t_{spd}$

As shown in Figure 6, at the moment after  $v_s$  turns to high voltage for switching on the transistor  $M_1$ , the parasitic capacitors in  $C_{oss}$  are discharged in order to bring the transistor  $M_1$  to the linear ohmic state. The capacitors  $C_{oss}$  discharge through the laser diode  $D_L$  and the inductor  $L_1$  with the governing equation as follows.

$$\frac{d^2 i_L}{dt^2} + 2\zeta_{spd}\omega_{spd} \frac{di_L}{dt} + \omega_{spd}^2 i_L = 0 \tag{18}$$

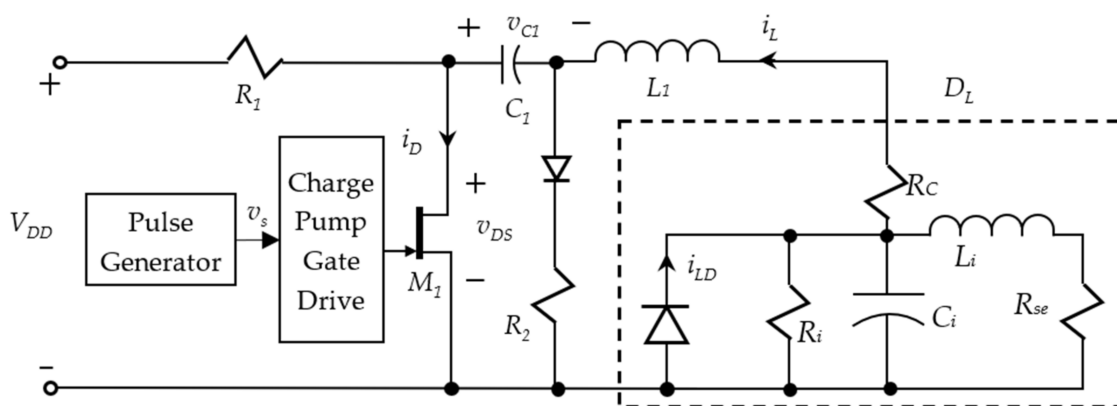


Figure 6. Laser driver circuit using D-mode GaN HEMT.

In the above equation, the natural frequency  $\omega_{spd}$  is a function of inductor  $L_1$  and capacitor  $C_{oss}$  as follows.

$$\omega_{spd} = \frac{1}{\sqrt{(L_1 + L_i)C_{oss}}} \tag{19}$$

The parallel resistance  $R_2$  can be ignored because the on-resistance of the GaN device is much smaller than  $R_2$ . However, the parallel resistance  $R_2$  may yield a current path when

the laser diode starts to flow and thus weaken the laser diode current. Therefore, we may add an extra diode to prevent  $R_2$  current from flowing in the same direction as the laser diode. The damping ratio of the current oscillation is as follows.

$$\zeta_{spd} = \frac{(R_C + R_{se})}{2} \sqrt{\frac{C_{oss}}{(L_1 + L_i)}} \tag{20}$$

where  $R_C$  is the contact resistance of the laser diode. The discharging is under a very light damping, hence the rise time of the current response, i.e., the discharging time, is estimated as follows.

$$t_{r,spd} = \frac{\pi}{\omega_{spd}} \tag{21}$$

According to the parameters of the inductance, parasitic capacitance, and the resistance provided as shown in Table 2, the capacitor discharging time together with the gate drive delay is, in total, around 1 ns. The switch parasitic capacitor discharge time  $t_{spd}$  forms a barrier for the laser current to flow; that is, the pulse duration shall not be smaller than  $t_{r,spd}$  in order to have the laser diode come to its stimulated emission.

**Table 2.** Parameters used in laser diode circuit modeling equations.

Symbol	Unit	Value
$C_{oss(GaN)}$	On Off	70 250
$R_C$ (Laser Diode)	mΩ	100
$R_{se}$ (Laser Diode)	mΩ	50
$L_1 + L_i$	nH	130
$\omega_{spd}$	Mrad/sec	332
$\zeta_{spd}$		0.001
$t_{r,spd}$	ns	9.5

### 3.3.2. Switch On-Time $t_{on}$

During the switch on-time, the switch conducts the current from the capacitor  $C_1$  through the laser diode  $D_L$  and the inductor  $L_1$  to the transistor  $M_1$  with the governing equation as follows. It is assumed that the diode holds a constant voltage  $V_{LD,on}$  depending on the  $I_{SS}$  of the laser diode. It may also be considered that the capacitor  $C_1$  charges both the inductor and the on-resistance of the transistor  $R_D$ . Assuming the on-resistance of the transistor  $R_D$  is small and the damping ratio  $\zeta_{on}$  is negligibly small, the governing equation is derived as follows.

$$\frac{d^2v_{C1}}{dt^2} + \omega_{on}^2 v_{C1} = 0 \tag{22}$$

In the above equation, the natural frequency  $\omega_{on}$  is a function of inductor  $L_1$  and capacitor  $C_1$  as follows.

$$\omega_{on} = \frac{1}{\sqrt{L_1 C_1}} \tag{23}$$

Substituting the initial voltage of  $v_{C1}$  as  $V_{C1} = V_{DD}$  into Equation (22), we obtain

$$v_{C1} = (V_{DD} - V_{LD,on}) \cos \omega_{on} t \tag{24}$$

The capacitor voltage of  $v_{C1}$  is reducing along the time when the transistor  $M_1$  is on, and the lost voltage of the capacitor will be refilled during the  $M_1$  turn-off time. The capacitor voltage drop when ignoring  $V_{LD,on}$  is derived as follows.

$$\Delta v_{C1} = V_{DD}(1 - \cos(\omega_{on} t_{on})) \tag{25}$$

The energy loss in the capacitor  $C_1$  is mainly consumed by the laser diode, hence the power transferred to the laser diode for the lighting pulse is then derived as follows.

$$P = \frac{C_1}{t_{on}} \left( V_{DD} - \frac{1}{2} \Delta v_{C1} \right) \Delta v_{C1} \tag{26}$$

The maximum power that can be transferred for each pulse can then be derived from taking the first derivative of the above equation.

$$\frac{d}{dt_{on}} P = C_1 V_{DD}^2 \frac{d}{dt_{on}} \frac{\left( \frac{1}{2} + \cos \omega_{on} t_{on} \right) (1 - \cos \omega_{on} t_{on})}{t_{on}} = 0 \tag{27}$$

One trivial solution of the above equation is  $t_{on} = \pi / \omega_{on}$ , that is, the electrical energy stored in the capacitor is used up during each pulse of laser switching. The inductor current  $i_{L1}$  is then derived in terms of the capacitor voltage as follows.

$$i_L = -L_1 \frac{dv_{C1}}{dt} = \omega_{on} L_1 (V_{DD} - V_{LD,on}) \sin \omega_{on} t \tag{28}$$

Although all current of  $i_L$  flows through the laser diode, only a portion of the current becomes the lighting current  $i_{LD}$  stated in Equation (1). The fraction between  $i_{LD}$  and  $i_L$  during the on-time is mainly a function of the resistance  $R_i$ , including the differential resistance of the laser diode model damping due to the spontaneous and stimulated recombination terms in the rate equations. The larger the resistance  $R_i$ , the higher the lighting current  $i_{LD}$  is. The other current branch of the laser diode includes the current path through the inductance  $L_i$ , representing the resonance phenomenon of the laser diode, the resistance  $R_{se}$ , representing damping due to spontaneous emission coupled into the lasing mode, and the current through the active layer diffusion capacitance of the laser diode  $C_i$ . The resonance phenomenon and the active layer diffusion will prolong the current of  $i_L$  after the lighting current  $i_{LD}$  cuts off from the diode equation.

The significance of this proposed circuit, obtained from Equation (22), is that there is no other resistor presented on the path of the laser diode lighting during the switch turn-on time. The damping ratio of the lighting current is subjected only to the dynamic on-resistance of the transistor  $M_1$ . When the on-resistance  $R_D$  of the transistor is made very small, the maximum light current is proportional to the  $V_{DD}$  and not limited by the resistance in the current loop.

### 3.3.3. Transistor Parasitic Capacitor Charge Time $t_{spc}$

As shown in Figure 6, at the moment after  $v_s$  turns to low voltage for switching off the transistor  $M_1$ , the parasitic capacitors in  $C_{oss}$  shall be charged in order to bring the transistor  $M_1$  to the off-state. The capacitors  $C_{oss}$  are charged through the laser diode  $D_L$  and the inductor  $L_1$  with the governing equation as follows.

$$\frac{d^2 i_L}{dt^2} + 2\zeta_{spc} \omega_{spc} \frac{di_L}{dt} + \omega_{spc}^2 i_L = 0 \tag{29}$$

In the above equation, the natural frequency  $\omega_{spc}$  and  $\zeta_{spc}$  are the same as  $\omega_{spd}$  and  $\zeta_{spd}$  derived in Equations (19) and (20), respectively. The charging is under a very light damping, hence the rise time of the current response, the charging time, is the same as derived in Equation (21). The only difference between charging and discharging of the parasitic capacitors is that the laser diode is conducting current  $i_{LD}$  during the charging time only.

$$t_{r,spc} = \frac{\pi}{\omega_{spc}} \tag{30}$$

During the same time, the current keeps flowing to drain out the zero-voltage junction capacitor of the laser diode, as shown in Figure 5.

### 3.3.4. Laser Diode Resonant Time $t_{lr}$

In the case where the GaN HEMT transistor  $M_1$  turns off at the time  $t_{r,spc}$  passed the  $v_s$  turn-off time, then the output parasitic capacitor  $C_{oss}$  of the transistor  $M_1$  has been filled up; however, the resonance through the same capacitor as the current in the inductor has no zero first-derivative.

$$\frac{d^2 i_L}{dt^2} + 2\zeta_{lr}\omega_{lr}\frac{di_L}{dt} + \omega_{lr}^2 i_L = 0 \tag{31}$$

The value of  $R_2$  is mapped into the dynamic impedance  $Z_2$  from the parallel connection with  $L_1$  and  $C_{oss}$  into a series connection as follows.

$$Z_2 = \frac{L_1 + L_i}{R_2(C_{oss(GaN,off)} + C_i)} \tag{32}$$

When the GaN HEMT transistor  $M_1$  turns off, the parallel resistance  $R_2$  can contribute to the damping ratio. The damping ratio  $\zeta_{lr}$  when  $R_C + R_{se} = Z_2$  is then written as follows.

$$\zeta_{lr} = \frac{(R_C + R_{se} + Z_2)}{2} \sqrt{\frac{C_{oss(GaN,off)} + C_i}{L_1 + L_i}} \approx \frac{1}{R_2} \sqrt{\frac{L_1 + L_i}{C_{oss(GaN,off)} + C_i}} \tag{33}$$

The damping ratio is preferable to be critical damping without causing too much turn-off overshoot voltage on  $v_{DS}$ . Table 3 shows the  $R_2$  adjusted according to the damping desired.

**Table 3.** Parameters for switch on-time.

Symbol	Unit	Value
$L_1$	nH	100
$L_i$	nH	30
$C_{oss(GaN,off)} + C_i$	pF	500
$R_C + R_{se}$	mΩ	200
$R_2$	Ω	8
$\zeta_{lr}$		2
		100
		0.16

### 3.3.5. $C_1$ Recovery Time

There is another important time that determines the repetition rate of the laser diode switching: the capacitor  $C_1$  recovery time. The recovery time is critical when the repetition rate increases, thus for the same pulse duration, the duty of the transistor switching increases. The supply of charges from resistor  $R_1$  through the path from  $R_1$  to  $C_1$  and then to  $R_2$  is activated only when the transistor turns off. The loss of charges from  $C_1$  during the transistor turn-on time must be refilled through its turn off time in order to maintain the capacitor  $C_1$  at the same voltage as the voltage source  $v_s$ . The time constant for the charging  $T_{c1}$  can be obtained from the RC charging equation as follows.

$$T_{c1} = (R_1 + R_2)C_1 \approx R_1C_1 \tag{34}$$

The capacitor  $C_1$  recovery time  $t_{c1r}$  may be estimated as four times the time constant  $T_{c1}$ , which is nearly 98% of the full voltage to  $V_{DD}$ .

### 3.4. Sensing the Laser Diode Current

In the small pulse duration or high repetition rate applications, it is difficult to directly measure either the current  $i_D$  or the voltage  $v_{DS}$  without interfering with the laser driver circuit. However, the state sensing is of extreme importance during the feedback control of the laser power. In Figure 7, we simplified the laser driver circuit from the view of resistor  $R_1$ . The resistor voltage is labeled in the opposite way such that it matches the wave form

of the supposed  $v_{DS}$ . In Figure 7a, the total laser diode current  $i_L$  can be obtained from the branch current solution as follows when  $R_1 \gg R_{D,on}$  is assumed.

$$i_L = \frac{V_{DD}}{R_{D,on}} - \frac{v_{R1}}{R_{D,on} || R_1} \approx \frac{V_{DD} - v_{R1}}{R_{D,on}} \tag{35}$$

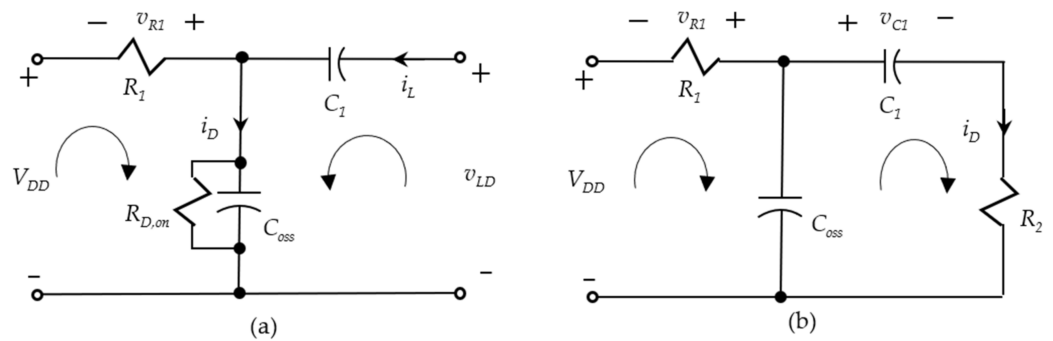


Figure 7. Resistor sensing (a) switch turn-on and (b) switch turn-off.

In the above equation, the input voltage  $V_{DD}$  is controlled through the power supply, the voltage  $v_{R1}$  is sensed, and the dynamic-on resistance of the transistor is assumed. In Figure 7b, the supplement voltage to the capacitor  $C_1$  is estimated.

$$\Delta v_{C1} = -\frac{\int_0^{t_{c1r}} v_{R1} dt}{R_1 C_1} = -\frac{\int_0^{t_{c1r}} v_{R1} dt}{T_{c1}} \approx -\frac{\int_0^{t_{c1r}} v_{R1} dt}{t_{c1r}/m} = -m \overline{v_{R1}} \tag{36}$$

The recovery time to time constant ratio  $m$  is suggested to be 4, as stated previously, when the 2% voltage error is considered to be the settling time clearance. The average voltage  $\overline{v_{R1}}$  on the resistor  $R_1$  can be estimated by taking the average of the integration.

Figure 8 shows the standard voltage response template on resistor  $R_1$ . With the voltage response, we can easily label the timing of the individual states of the laser driving process. The anomaly cases include:

- (a) Due to either the resistance of  $R_1$  being too high or the capacitance  $C_1$  being too small, the voltage of  $v_{R1}$  is below zero voltage all the time during the high repetition rate operation.
- (b) The voltage of  $v_{R1}$  does not fall to  $-V_{DD}$  during the short pulse duration operation.
- (c) Due to either the damping of the laser driver circuit being too high or the charge pump gate drive being subjected to high gate resistance, the voltage of  $v_{R1}$  does not oscillate during the laser diode resonant time  $t_{lr}$ .

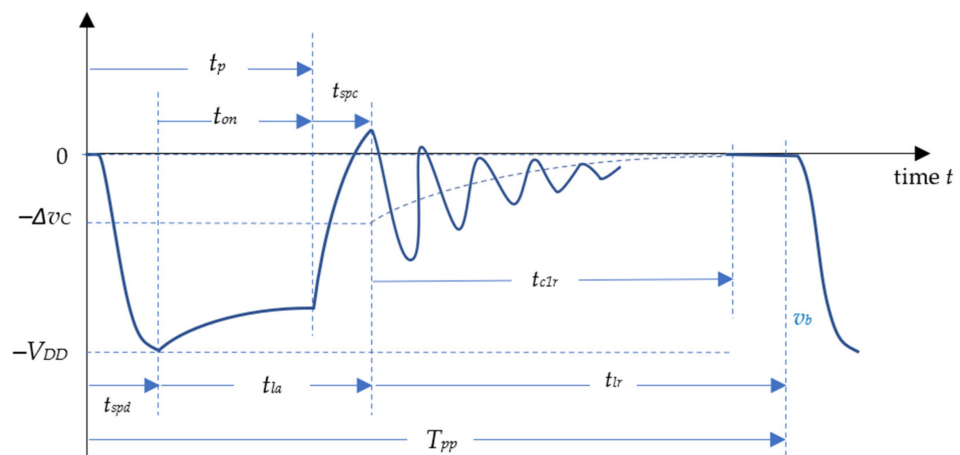


Figure 8. Voltage response of resistor  $R_1$ .

#### 4. Design Guide

The parameter used in the proposed circuit consists of mainly the input voltage to the laser diode driver  $V_{DD}$ , which is controlled by the power supply, as stated previously. In order to maintain the correct voltage, the duty cycle ( $\delta_b$ ) is controlled as stated in Equation (13). The other parameters, including the resistor  $R_1$  for both experimental sensing and the charging of capacitor  $C_1$  and the capacitance  $C_1$ , are critical to the power efficiency, maximum pulse duration, and peak laser lighting power.

##### 4.1. Power to Light Efficiency

As shown in Figure 8, there are mainly two sessions of the power losses from the resistor  $R_1$  as follows. The first session of power loss is due to the current conducting through  $R_1$  to  $M_1$  during the transistor  $M_1$  turn-on time. The joule loss from  $R_1$  is estimated by assuming the on-resistance of the transistor  $R_D$  is small as follows.

$$J_{L,on} = \frac{V_{DD}^2}{R_1} t_{on} \tag{37}$$

The second session of power loss is to refill the capacitor  $C_1$  to again reach the voltage  $v_{C1}$ . The joule loss from  $R_1$  during the transistor  $M_1$  turn-off time is derived from the integration of the exponential current charging of the capacitor  $C_1$ .

$$J_{L,off} = \int (\Delta v_{C1} e^{-t/(R_1 C_1)}) \times \frac{\Delta v_{C1} e^{-t/(R_1 C_1)}}{R_1} dt = \frac{C_1 \Delta v_{C1}^2}{2} \tag{38}$$

The voltage loss  $\Delta v_{C1}$  in capacitor  $C_1$  is due to the lighting, and the remaining voltage is derived in Equation (25), which is proportional to  $v_{C1}$ . The electrical power loss of the laser diode driver is then derived as follows.

$$P_L = \frac{J_{L,on} + J_{L,off}}{T_{pp}} \tag{39}$$

where  $T_{pp}$  is defined previously as the repetition period, which is the reciprocal of the repetition rate  $f_{LD}$ . The electrical power loss is proportional to the repetition rate as well as the square of the voltage  $V_{C1}$ . In order to reduce the electrical power loss, we will need to (a) reduce the capacitance  $C_1$  and (b) increase the resistance  $R_1$ . The lighting current  $i_{LD}$  is proportional to  $v_{C1}$  and the laser diode voltage holds constant  $V_{LD,on}$ . Therefore, the power to light efficiency is in proportion to the product of the repetition rate and the  $V_{DD}$ .

$$\eta \propto \frac{1}{f_{LD} V_{DD}} \tag{40}$$

##### 4.2. Maximum Pulse Duration and Repetition Rate $f_{LD}$

Because the lighting current  $i_{LD}$  of the laser diode will turn off when the current reverses, as shown in Figure 6, the maximum pulse duration  $t_{p,max}$  is restrained by Equation (28) and  $i_L > 0$  as follows.

$$t_p < t_{p,max} = \frac{\pi}{\omega_{on}} = \pi \sqrt{L_1 C_1} \tag{41}$$

In order to have a small pulse duration, we will need to decrease either the parasitic inductance  $L_1$  or the capacitance  $C_{oss(GaN,on)} + C_i$ . It will need four times the time constant  $R_1 C_1$  to recover the capacitor  $C_1$  back into  $V_{DD}$ ; therefore, the repetition rate is limited by the reciprocal of  $R_1 C_1$  as follows.

$$f_{LD} < \frac{1}{4R_1 C_1} \tag{42}$$

In order to increase the repetition rate, we will need to decrease both  $R_1$  and  $C_1$ .

### 4.3. Peak Power

The peak power is determined by the electrical energy storage in the capacitor as follows.

$$P_{LD} \propto \frac{1}{t_p} \int V_{LD,on} di_L \gg \frac{1}{2} C_1 V_{DD}^2 \frac{1 - \cos \omega_{on} t_p}{t_p} \tag{43}$$

Substituting  $t_p$  as its maximum value  $t_{p,max}$  from Equation (41), we obtain the  $P_{LD}$  follows.

$$P_{LD} \propto V_{DD}^2 \sqrt{\frac{C_1}{L_1}} \tag{44}$$

In order to increase the peak power of laser lighting, we will need to increase the input voltage  $V_{DD}$  and  $C_1$  as well; however, we can also decrease  $L_1$  to increase the peak power.

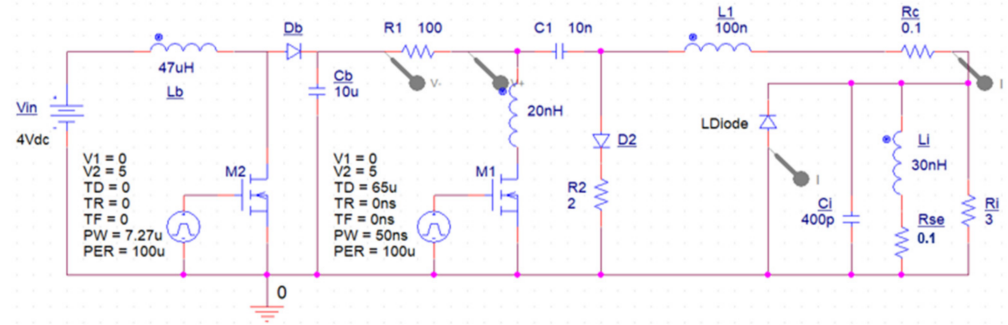
Table 4 summarizes the design guide for different purposes of the applications; all agree that the inductance  $L_1$  is to be minimized. Except for the high peak power of laser output, the capacitance  $C_1$  is preferred to be small. In order to increase the repetition rate, we will have to choose a low resistance  $R_1$ . In order to increase peak power of the laser output, we will need to increase the input voltage  $V_{DD}$ .

**Table 4.** Design guide of the proposed laser driver circuit.

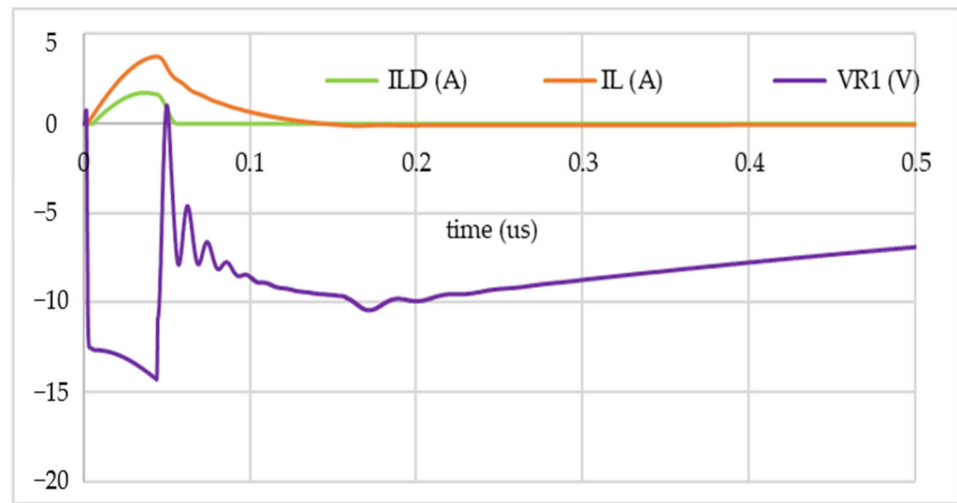
Task	Preference			
	$V_{DD}$	$R_1$	$C_1$	$L_1$
Increase repetition rate $f_{LD}$		decrease	decrease	
Decrease pulse duration $t_{p,max}$			decrease	decrease
Increase peak power $P_{LD}$	increase		increase	decrease
Increase power to light efficiency $\eta$	decrease	increase		

### 5. Simulation and Experiment

The laser diode SPICE model is based on the laser diode model specified in Table 1. The boost power supply on the left part of the PSPICE circuit model, shown in Figure 9a, is so operated that the  $V_{DD}$  shown in capacitor  $C_b$  is 15 V while the simulation result for  $t_p = 50$  ns at its steady state is shown in Figure 9b. There is a parasitic inductance due to bonding connected in series with the transistor  $M_1$ . The parameters used in the simulation as experiment as well are shown in Table 5. The  $\omega_{on}$  derived in Equation (23) is also calculated and converted to 5 MHz, as shown Table 5. The maximum pulse duration  $t_{p,max}$  is calculated from Equation (41) as 100 ns. The pulse duration  $t_p = 50$  ns is half of  $t_{p,max} = 100$  ns; one half of total electrical energy previously stored in the capacitor  $C_1$  was released during the laser light process. Therefore, the  $\Delta v_{C1}$  is calculated as  $0.3V_{DD} = 4.5$  V from Equation (25) when the switch parasitic capacitor discharge time  $t_{spd}$  is negligibly small and  $t_{on} \approx t_p$ . The simulation result shows, in Figure 9b, the voltage  $v_{R1}$  (purple curve line) measured on the resistor  $R_1$  goes from 0 V at 0 s representing the  $M_1$  turn-off state, immediately drops down to  $-V_{DD}$  representing when the transistor  $M_1$  turns on, then jumps to 0 V again at 50 ns, indicating the transistor has been turned off again, and later falls back to the voltage  $-(V_{DD} - \Delta v_{C1}) = -10$  V at 150 ns, which is inconsistent with the result predicted in Equation (25). For a shorter pulse duration, say, one-tenth of 100 ns ( $t_{p,max}$ ), the repetition rate can be as high as 10 MHz.



(a)



(b)

Figure 9. PSPICE simulation (a) circuit and (b) result for pulse duration 50 ns.

Table 5. Parameters for laser diode driver simulation and experiment.

Symbol	Unit	Value
$L_1$	nH	100
$C_1$	nF	10
$R_1$	$\Omega$	100
$\omega_{on}$	Mrad/s	31.6
$t_{p,max}$	ns	100
$f_{on} = \omega_{on}/2\pi$	MHz	5

For estimating the output power of a laser diode, the photodiode detector DET08CL(/M) is used, which is an InGaAs junction photodiode (an intrinsic device), and a 50  $\Omega$  terminator is used in conjunction with a 50  $\Omega$  coaxial cable in our measurements. It behaves similarly to an ordinary signal diode, but it generates a photocurrent when light is absorbed in the depleted region of the junction semiconductor. It determines the expected level of the output current ( $I_{OUT}$ ) and the responsivity based upon the incident light.

$$I_{OUT} = I_{DARK} + I_{PD} \cong I_{PD} \tag{45}$$

The definition of photodiode responsivity  $R(\lambda) = I_{PD}/P$  is the ratio of generated photocurrent  $I_{PD}$  to the incident light power  $P$  at a given wavelength  $\lambda$ . According to the response curve, the photodiode responsivity  $R(\lambda)$  is around 0.6 A/W at wavelength 940 nm. Ignoring the dark current ( $I_{DARK}$ ), junction capacitance ( $C_j$ ), and the other electric characters in the circuit, the received power can be carried out via measured photocurrent ( $I_{PD}$ ) at wavelength 940 nm.

$$P = \frac{I_{PD}}{R(\lambda)@940nm} \cong \frac{I_{PD}}{0.6} \tag{46}$$

To estimate the total out power of the laser diode, the diverging solid angle of the laser beam is checked, and the solid angle of the photodetector is calculated from the active area diameter. The solid angle of a cone with its apex at the apex of the solid angle, and with the full divergence angle  $2\theta$ , is the area of a spherical cap on a unit sphere. The value of  $\theta$  defined in this paper is the half angle of the beam plane.

$$\Omega = \int_0^{2\pi} \int_0^\theta \sin \theta d\theta d\phi = 2\pi(1 - \cos \theta) = 4\pi \sin^2 \frac{\theta}{2} (\text{steradian}) \tag{47}$$

For the PCSEL L13395-04 (HAMAMATSU), its beam spread angle is only 1 degree when its operating power is around 150 mW,  $\Delta\Omega \cong 9.70 \times 10^{-5} (\text{steradian})$ . For a 940 nm VCSEL V3-7-2000-S (EGISMOS), its beam spread angle along the wide axis is 60 degrees and is 45 degrees along the narrow axis,  $\Delta\Omega \cong 0.24 (\text{steradian})$ .

The photodiode detector for the experiment and the experimental setup are shown in Figures 10 and 11, respectively. In the experiment, we used the 940 nm VCSEL fabricated in the Department of Photonics at NYCU. The  $V_{DD}$  in this experiment is 15 V. The prototyping board is used in the experiment, and the parasitic inductance  $L_1$  is approximately 100 nH according to the model fitting of the frequency response using Equation (22). The thickness of the prototyping board is 1.55 mm. The spacing between the VCSEL and the photodiode detector is 5 mm, which can also be observed from the Figure 11a side view to compare the thickness with the distance. The active area diameter of the DET08CL(/M) InGaAs junction photodiode is  $\varnothing 80 \mu\text{m}$ , and its received solid angle was calculated as follows when  $\theta \cong \sin^{-1}(80\mu\text{m}/5\text{mm}) \approx 0.016\text{rad}$ .

$$\Delta\Omega = 4\pi \sin^2 \frac{\theta}{2} \cong 8 \times 10^{-4} (\text{steradian}) \tag{48}$$

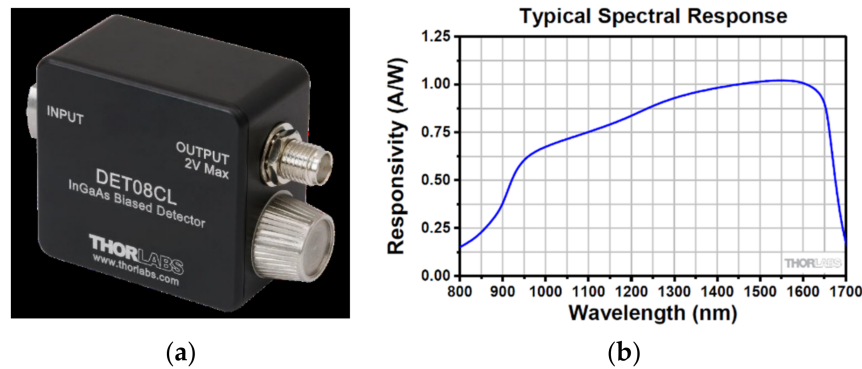


Figure 10. (a) Photodiode detector for the experiment and (b) corresponding responsivity.

The power correcting factor for a 940 nm VCSEL V3-7-2000-S is around 300. As for the PCSEL L13395-04, the estimated received power does not have to be corrected because its divergence solid angle is smaller than that of the DET08CL. The D-mode GaN HEMT is used in the experiment, as shown in Figure 11b, as the transistor  $M_1$ . We used a 10 nF capacitor  $C_1$  to produce a  $t_{p,max} = 100$  ns pulse, which is inconsistent with the simulation. The result is shown in Figure 12. In Figure 12, there are four curves. The first curve, in blue, is the gate-source voltage  $v_{GS}$  of the D-mode GaN HEMT. Because the D-mode GaN HEMT is a normally on device and the turn-on voltage of the D-mode GaN HEMT is  $-7$  V, a charge pump gate drive is used, as shown in Figure 6. The second curve, in green, is the drain-source voltage  $v_{DS}$  response of the D-mode GaN HEMT. We directly measured the  $v_{DS}$  using a difference voltage probe that has very low capacitance. The third curve, in purple, is the  $v_{RI}$ . As stated in Section 3.4, the voltage response of  $v_{RI}$  is

similar to  $v_{DS}$ , with the only difference being in voltage shift. Comparing  $v_{R1}$  in 4 V/div and  $v_{DS}$  in 10 V/div from the experimental result, we actually found the  $v_{R1}$  is oscillating more than  $v_{DS}$  and with some amount of delay. The fourth curve, in cyan is the current taken from the photodetector, and the peak ampere is 165 mA. According to the power correcting factor calculated from 5 mm distance according to Equation (48) and the power conversion according to Equation (46), the peak power is calculated to be 81 W. It is also observed from Figure 12 that there is still some amount of residual laser light showing on the photodetector, which may be due to the VCSEL resonance.

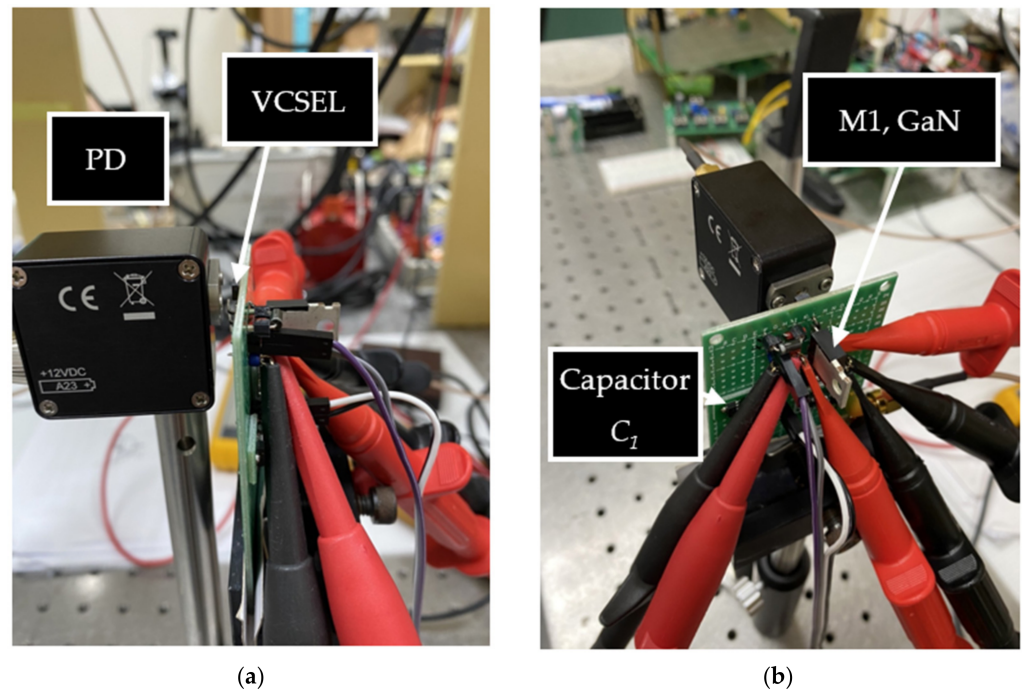


Figure 11. Experiment setup: (a) side view and (b) front view.

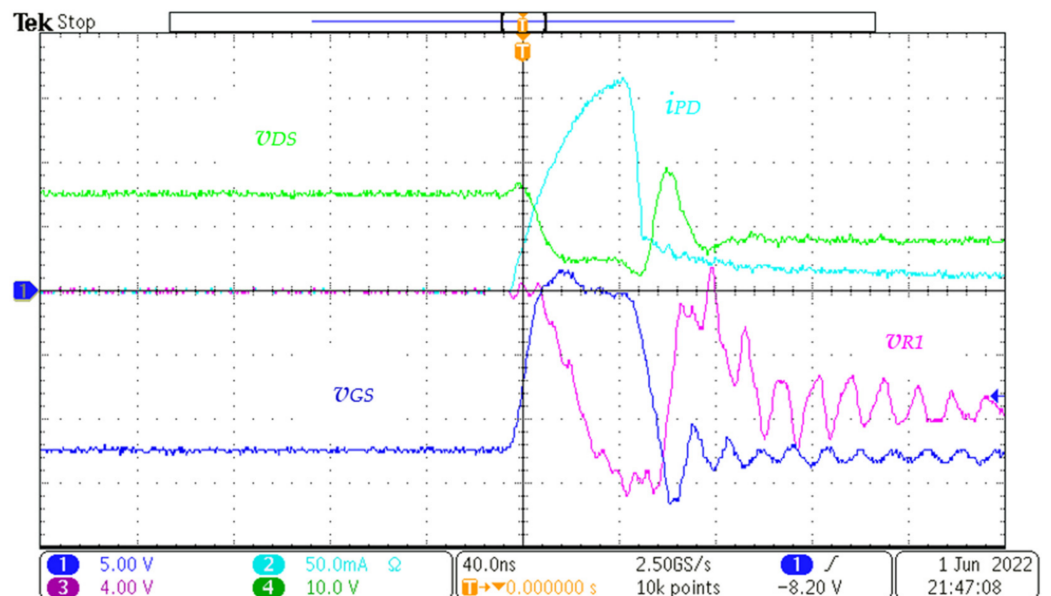
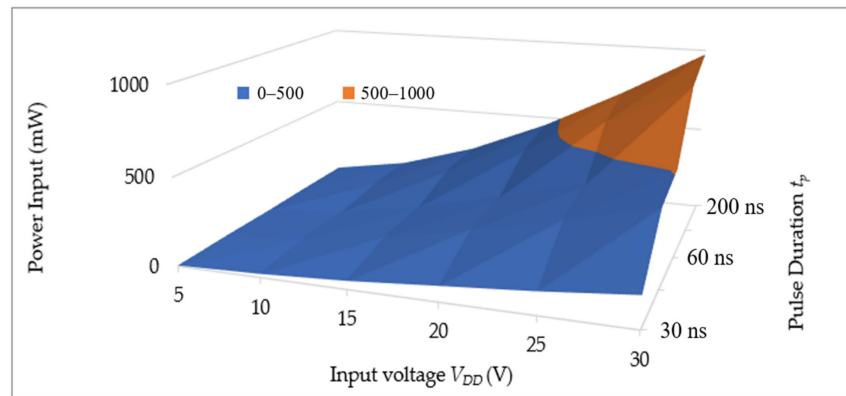


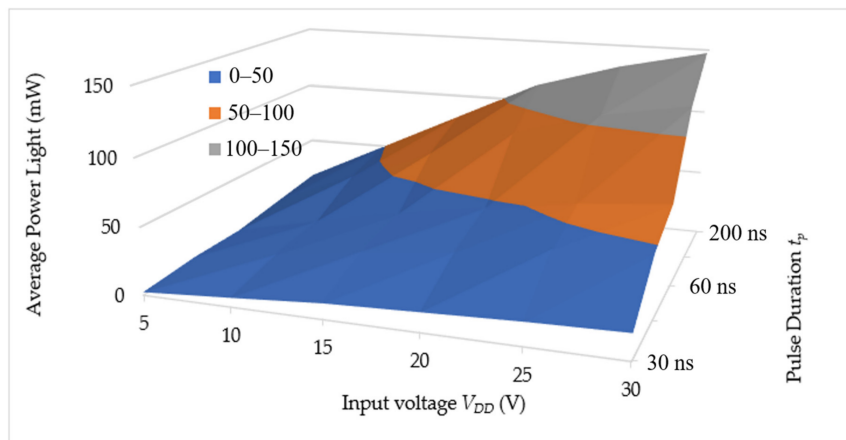
Figure 12. Result of Appendix A: the experiment with 50 ns pulse duration.

The performance measurement is summarized from many more experiments on the same experiment setup as shown in Figure 11. The input power measured from the

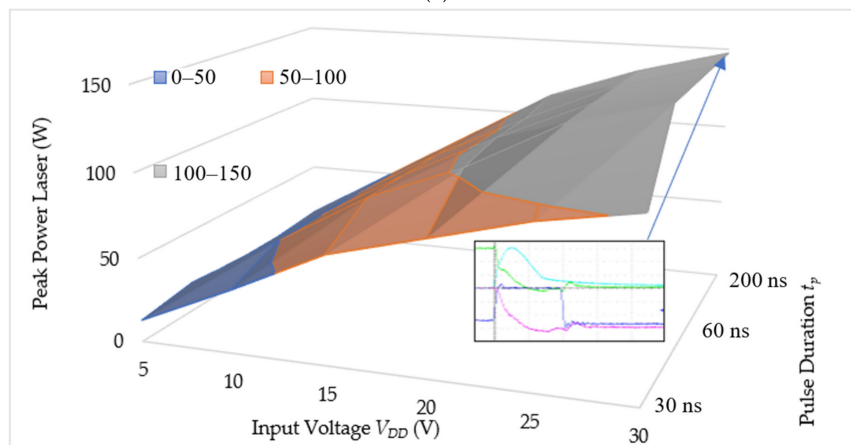
power supply reading is shown in Figure 13a. The average lighting power is shown in Figure 13b. The peak power shown in Figure 13c is inconsistent with the power estimated in Equation (44): the higher the input voltage to the laser driver, the larger the peak power from the laser is. The efficiency from the electrical power input to the average laser output power is shown in Figure 13d, which is inconsistent with Equation (40): the lower the input voltage, the higher the efficiency is. As a result, calculated from the experiments, we conclude that, for the current implementation, the highest efficiency is 86% and the maximum power is 150 W. Both the efficiency and the peak power stands for the turn-on time  $t_{on}$ , which should be no less than the pulse duration  $t_{p,max}$ . In Figure 12, it is observed that when  $t_{on}$  is larger than  $t_{p,max}$ , the pulse duration remained at  $t_{p,max} = 100$  ns when ignoring the residual light.



(a)



(b)



(c)

Figure 13. Cont.

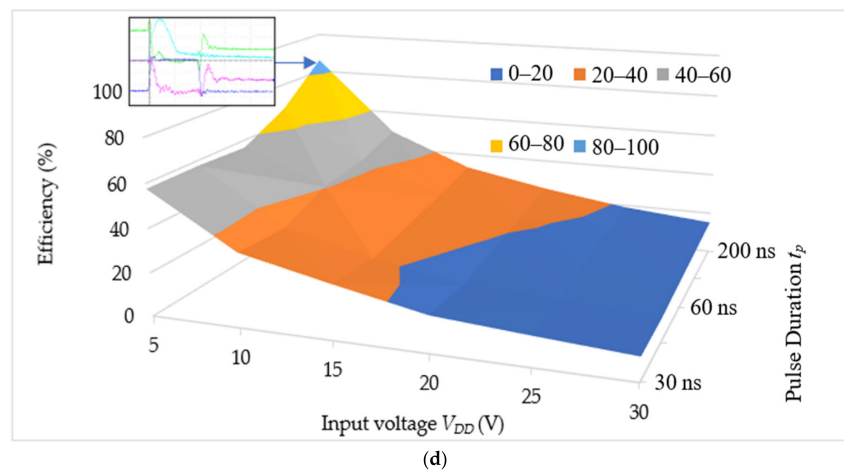


**Figure 13.** The performance indices: (a) electrical power input, (b) average laser power output, (c) laser peak power, and (d) efficiency with waveforms (green:  $v_{DS}$ , cyan:  $i_{PD}$ , blue:  $v_{GS}$ , purple:  $v_{R1}$ ).

### 6. Discussion

When the VCSEL (around 30~40%) efficiency is unknown, the direct measurement, which imposed extra measurement inductance and capacitance on the VCSEL, is inappropriate for calculating the output power; therefore, we estimated the output power of a laser diode using the photodiode detector (PD) DET08CL. A standard method, such as the integrating sphere, collects electromagnetic radiation from a source completely external to the optical device and can be used to precisely measure the output power of the VCSEL laser. Other methods that split the optical beam into two branches [23]—one is directed to an optical spectrum analyzer (OSA), and the other to the optical input of an oscilloscope—may also be used to measure the output power of the VCSEL laser. Although PD is not the best component for the absolute measurement mean, for the circuit designer it is simple and can provide enough relative information for the circuit designer to understand the relationships among the repetition rate, pulse duration, and the laser output power.

There are state-of-the-art commercial drivers for laser diode that can output higher repetition and short pulse duration, such as those from Analog Modules, Inc. (Longwood, Orlando, USA) Model 7612 A [29] is capable of 1.25 W, 10 ns pulse width, and 50 MHz repetition rate. The driver circuit of this paper is oriented to yield a large instantaneous laser power output in an efficient way. The design specifications include a pulse duration of 10~100 ns and a 10 MHz repetition rate when the peak power is 100W. The high instantaneous laser power is due to our circuit design, as shown in Figure 6. Our driver uses the D-mode GaN HEMT, which has a very small  $C_{oss}$  difference between turn-on and turn-off states, and which is used to drive the VCSEL made in NYCU. There are still areas for improvement, such as circuit fabrication, SiP (system in a package) IC design, and VCSEL efficiency, to be achieved in order to catch up with those state-of-the-art products.

The key factors of the output stability in the experiment include the stray inductance due to the wiring path of the laser diode (VCSEL in this study), the input parasitic capacitance  $C_{iss}$  of the GaN HEMT, and the cooling of the circuit board. Among these factors, the stray inductance is most critical factor. Extra stray inductance may result in reduction of the maximum output current and the maximum laser output power, which can be improved through shortening the current path from the laser to the capacitor  $C_1$  and to the transistor  $M_1$ . Thus, flip-chip bonding instead of wire bonding is recommended for future work. The input parasitic capacitance is critical to achieve shorter pulse duration as well as higher repetition rate, which can be reduced by fabricating the GaN HEMT with a smaller gate width. A 20 mm GaN HEMT device will be introduced to replace the 120 mm device used in this paper, of which the differences between the devices and the laser output characteristics will be reported in future work. The copper pours, the clip bond, and the ribbon bond are

solutions to enhance the heat dissipation of the laser diode driver circuit, which actually help the laser output stability.

## 7. Conclusions

A laser diode driver circuit is proposed in this paper, which has the advantages that only a single Li-ion battery is needed to provide the adjustable voltage to the laser diode driver, as well as that feedback control can be achieved through the resistor voltage reading without interfering with the current path of laser lighting. The other advantage is its high peak power due to the parallel topology for the power input and the laser emitting. In this paper, the mathematical model of the laser driver is derived according to the laser driver topology to yield the preliminary parameter design of the electronic components. In the experiment, we used the 940 nm VCSEL fabricated in the Dept. of Photonics at NYCU. The circuit model of the VCSEL made at NYCU was acquired by comparing the results between the experiments and the PSPICE simulation. With the SPICE circuit model, we then derived the design guide for different application purposes. The results of a power efficiency of 86% and a maximum peak power of 150 W were obtained for the flash LiDAR application. It will still need further improvement through fabricating the GaN HEMT at NCTU with smaller parasitic capacitances and reducing the parasitic inductance on the circuit board for future application of the VCSEL as the laser emitter on the LiDAR system, which needs a repetition rate as high as 25 MHz with a pulse duration as short as 5 ns.

**Author Contributions:** Conceptualization, H.-C.K., E.-Y.C. and W.-H.C.; methodology, C.-C.W.; software, C.-C.W.; validation, C.-Y.L. and C.-Y.P.; formal analysis, L.-C.T.; writing—original draft preparation, W.-H.C.; writing—review and editing, C.-Y.L. and C.-C.W.; visualization, C.-Y.L. and C.-C.W.; supervision, E.-Y.C.; project administration, W.-H.C. and L.-C.T.; funding acquisition, H.-C.K., W.-H.C. and E.-Y.C. All authors have read and agreed to the published version of the manuscript.

**Funding:** This research was funded in parts by Ministry of Science and Technology, R.O.C., grant number MOST(NSC) 110-2622-8-A49-008-SB and MOST(NSC) 111-2218-E-008-006.

**Institutional Review Board Statement:** Not applicable.

**Informed Consent Statement:** Not applicable.

**Data Availability Statement:** Not applicable.

**Acknowledgments:** This work was supported by the Ministry of Science and Technology, R.O.C. The authors also thank You-Chen Weng of the CSD Lab for fabricating the D-Mode MIS-HEMT chips and IMLab graduate students for their help in the experimental setup.

**Conflicts of Interest:** The authors declare no conflict of interest.

## Appendix A

**Table A1.** The specifications of electronic components in Figure 9.

Designator	Part Description	Manufacturer	Manufacturer Part #
$L_b$	IC, Gate driver Inductor, 47 $\mu$ H	Texas Instruments TDK	LM5114BMF/NOPB SLF12575T-470M2R7-PF
$M_2$	Transistor, Cascode GaN Type 2B	NYCU [17]	
$D_b$	Fast recovery diode, 200 V, 10 A	ROHM semiconductor	RFN10T2D
$C_b$	Capacitor, 10 $\mu$ F, 50 V, X5R 0805	Murata	GRM21BR61H106KE43L
$R_1$	Resistor, 100 $\Omega$ , $\pm$ 1%, 1/8W, 0805	Yageo	RC0805FR-07100RL

Table A1. Cont.

Designator	Part Description	Manufacturer	Manufacturer Part #
$M_1$	Transistor, depletion mode GaN HEMT with charge pump circuit	NYCU [16,17]	
$C_1$	Capacitor, 100 nF, 50 V, X7R 0805	Murata	GCD21BR71H104KA01L
$D_2$	Fast recovery diode, 200 V, 0.5 A	ROHM semiconductor	RF05VYM2SFHTR
$R_2$	Resistor, 2 $\Omega$ , $\pm 5\%$ , 1/8 W, 0805	Yageo	RC0805JR-072RL
$D_L$	VCSEL, 940 nm 2 W	Egismos	V3-7-2000-S

## References

- Lemmetti, J.; Sorri, N.; Kallioniemi, I.; Melanen, P.; Uusimaa, P. Long-Range All-Solid-State Flash LiDAR Sensor for Autonomous Driving. In *High-Power Diode Laser Technology XIX*; Zediker, M.S., Ed.; SPIE: California, CA, USA, 2021.
- Wallace, L.; Lucieer, A.; Watson, C.; Turner, D. Development of a UAV-LiDAR System with Application to Forest Inventory. *Remote Sens.* **2012**, *4*, 1519–1543. [CrossRef]
- Dassot, M.; Constant, T.; Fournier, M. The Use of Terrestrial LiDAR Technology in Forest Science: Application Fields, Benefits and Challenges. *Ann. For. Sci.* **2011**, *68*, 959–974. [CrossRef]
- McManamon, P.F. *Field Guide to Lidar*; SPIE: Bellingham, WA, USA, 2015.
- Ismail, H.; Roy, R.; Sheu, L.-J.; Chieng, W.-H.; Tang, L.-C. Exploration-Based SLAM (e-SLAM) for the Indoor Mobile Robot Using Lidar. *Sensors* **2022**, *22*, 1689. [CrossRef] [PubMed]
- Wens, M.; Redoute, J.-M.; Blanchaert, T.; Bleyaert, N.; Steyaert, M. An Integrated 10A, 2.2ns Rise-Time Laser-Diode Driver for LIDAR Applications. In *2009 Proceedings of ESSCIRC*; IEEE: Athens, Greece, 2009.
- Glaser, J. High Power Nanosecond Pulse Laser Driver Using an GaN FET. In Proceedings of the PCIM Europe 2018, International Exhibition and Conference for Power Electronics, Intelligent Motion, Renewable Energy and Energy Management, Nuremberg, Germany, 5–7 June 2018; pp. 1–8.
- ROHM Semiconductor. Laser Diode Drive Circuit Design Method and Spice Model. December 2020. Rev.002. Appl. Note No. 63AN147E. Available online: [https://fscdn.rohm.com/en/products/databook/applinote/opto/laser\\_diode/high\\_power/ld\\_for\\_lidar\\_spice\\_an-e.pdf](https://fscdn.rohm.com/en/products/databook/applinote/opto/laser_diode/high_power/ld_for_lidar_spice_an-e.pdf) (accessed on 1 March 2022).
- Nissinen, J.; Kostamovaara, J. A high repetition rate CMOS driver for high-energy sub-ns laser pulse generation in SPAD-based time-of-flight range finding. *IEEE Sens. J.* **2016**, *16*, 1628–1633. [CrossRef]
- Tajfar, A.; Zamprogno, M.; Villa, F.; Zappa, F. A 20 A Sub-Nanosecond Integrated CMOS Laser Diode Driver for High Repetition Rate SPAD-Based Direct Time-of-Flight Measurements. In Proceedings of the International Conference on Computing Electronics & Communications Engineering (iCCECE), Southend, UK, 16–17 August 2018; pp. 272–276.
- Arslan, S.; Shah, S.A.A.; Kim, H. Power Efficient Current Driver Based on Negative Boosting for High-Speed Lasers. *Electronics* **2019**, *8*, 1309. [CrossRef]
- Glaser, J. How GaN Power Transistors Drive High-Performance Lidar: Generating Ultrafast Pulsed Power with GaN FETs. *IEEE Power Electron. Mag.* **2017**, *4*, 25–35. [CrossRef]
- Svilainis, L.; Chaziachmetovas, A.; Eidukynas, V.; Aleksandrovas, A.; Varatinskas, M. Compact Laser Driver for Ultrasonic Arbitrary Position and Width Pulse Sequences Generation. *IEEE Trans. Instrum. Meas.* **2021**, *70*, 1–15. [CrossRef]
- Efficiency Power Conversion. Development Board EPC9144 Quick Start Guide. 2019. Rev.1.0. Available online: [https://epc-co.com/epc/Portals/0/epc/documents/guides/EPC9144\\_qsg.pdf](https://epc-co.com/epc/Portals/0/epc/documents/guides/EPC9144_qsg.pdf) (accessed on 4 March 2022).
- Zhang, Y.; Yang, F. *Maximizing the Performance of GaN with Ideal Diode Mode*; Texas Instruments Application Report; Texas Instruments: Dallas, TX, USA, 2020.
- Weng, Y.-C.; Wu, C.-C.; Chang, E.-Y.; Chieng, W.-H. Minimum Power Input Control for Class-E Amplifier Using Depletion-Mode Gallium Nitride High Electron Mobility Transistor. *Energies* **2021**, *14*, 2302. [CrossRef]
- Wu, C.-C.; Liu, C.-Y.; Anand, S.; Chieng, W.-H.; Chang, E.-Y.; Sarkar, A. Comparisons on Different Innovative Cascode GaN HEMT E-Mode Power Modules and Their Efficiencies on the Flyback Converter. *Energies* **2021**, *14*, 5966. [CrossRef]
- Ben-Yaakov, S.; Van de Perre Sr, L. A Novel Circuit Topology for Turning a ‘Normally On’ GaN Transistor into ‘Normally Off’ that Can be Driven by Popular Drivers. In *Bodo’s Power Systems*; 2018; pp. 96–99. Available online: <https://www.ee.bgu.ac.il/~pel/pdf-files/jour147.pdf> (accessed on 19 June 2022).
- Peftitsis, D.; Rabkowski, J.; Nee, H.-P. Self-Powered Gate Driver for Normally ON Silicon Carbide Junction Field-Effect Transistors Without External Power Supply. *IEEE Trans. Power Electron.* **2012**, *28*, 1488–1501. [CrossRef]
- Park, M.; Baek, Y.; Dinare, M.; Lee, D.; Park, K.-H.; Ahn, J.; Kim, D.; Medina, J.; Choi, W.-J.; Kim, S.; et al. Hetero-integration enables fast switching time-of-flight sensors for light detection and ranging. *Sci. Rep.* **2020**, *10*, 1–8. [CrossRef] [PubMed]

21. Liu, A.; Wolf, P.; Lott, J.A.; Bimberg, D. Vertical-cavity surface-emitting lasers for data communication and sensing. *Photonics Res.* **2019**, *7*, 121–136. [[CrossRef](#)]
22. Haghghi, N.; Moser, P.; Lott, J.A. Power, bandwidth, and efficiency of single VCSELs and small VCSEL arrays. *IEEE J. Sel. Top. Quantum Electron.* **2019**, *25*, 1–15. [[CrossRef](#)]
23. Rosado, A.; Vilera-Suarez, M.F.; Perez-Serrano, A.; Tijero, J.M.G.; Esquivals, I. Characterization of optical pulses generated by gain switching a 1310 nm vcsel. In *OPTOEL 2017; SEDOPTICA*: Santiago de Compostela, Spain, 2017.
24. Hogan, B. Operation of VCSELs under Pulsed Conditions Increasing VCSEL Output Power. January 2010. Vixar, Appl. Note. Available online: <https://www.auniontech.com/ueditor/file/20170921/1505977465336422.pdf> (accessed on 21 January 2010).
25. Zhou, G.; Yang, J.; Li, X.; Yang, X. Advances of flash LiDAR development onboard UAV. *ISPRS-Int. Arch. Photogramm. Remote Sens. Spat. Inf. Sci.* **2012**, *39*, 193–198. [[CrossRef](#)]
26. Lim, D.W.; Cho, H.U.; Sung, H.K.; Yi, J.C. A PSPICE circuit modeling of strained AlGaInN laser diode based on the multilevel rate equations. *J. Opt. Soc. Korea* **2009**, *13*, 386–391. [[CrossRef](#)]
27. Bera, S.C.; Singh, R.V.; Garg, V.K. A temperature dependent PIN diode model for simple temperature invariant attenuator circuits. *Microw. J.* **2005**, *48*, 104–106.
28. Madhan, M.G.; Rekha, E.; RajKumar, P. A Comprehensive Equivalent Circuit Model for the Study of Thermal and Spectral Characteristics in Laser Diodes. *Optik* **2014**, *125*, 3030–3036. [[CrossRef](#)]
29. Semiconductor Optical Amplifier Driver Assembly Model 7612A. ANALOG MODULES, INC., Appl. Note. Available online: <http://analogmodules.com/wp-content/uploads/7612A.pdf> (accessed on 9 September 2022).